

Figure 1 Enzymatic CYP induction by β -carotene. Male Sprague-Dawley rats (aged 6–7 weeks, 140 \pm 10 g) maintained on a standard laboratory diet received by mouth daily 500 mg per kg body weight of β -carotene (Aldrich, Milan) for five consecutive days; controls received only corn oil. Because of species specificity, the purpose of the *in vivo* experiments was to find evidence of the co-carcinogenic potential of β -carotene⁷, not to mimic a trial situation. Rats were fasted for 16 h before being killed humanely in accordance with approved procedures. Ten rats were in each group; lung microsomes were tested immediately for ethoxyresorufin *O*-deethylase (EROD) and testosterone hydroxylase⁸ (TH).

Because β -carotene is known to be an anti-genotoxic agent⁶, we decided to investigate whether it might act by means of epigenetic mechanisms, such as those involving cytochrome P450 (CYP) changes⁷.

We found a highly significant increase in the carcinogen-metabolizing enzymes CYP1A1/2 (activating aromatic amines, polychlorinated biphenyls, dioxins and PAHs), CYP3A (activating aflatoxins, 1-nitropyrene and PAHs), CYP2B1 (activating olefins and halogenated hydrocarbons) and CYP2A (activating butadiene, esamethyl phosphoramidate and nitrosamines) in the lungs of rats supplemented with high doses of β -carotene. This was documented by marked increases in the following probes: ethoxyresorufin *O*-deethylase activity (CYP1A1-linked), testosterone 7 α -hydroxylation (CYP1A1/2 and CYP2A1), 6 β -hydroxylation (CYP1A1/2 and CYP3A1), 2 β -hydroxylation (CYP1A1 and CYP3A1) and androst-4-ene-3,17-dione-associated monooxygenase (17-testosterone hydroxylase, CYP2B1 and CYP3A1) (Fig. 1).

In humans, correspondingly high levels of CYPs would predispose an individual to cancer risk from the widely bioactivated tobacco-smoke procarcinogens. Moreover, many of these could act synergistically with β -carotene as CYP inducers to impose a co-carcinogenic effect, particularly in genetically predisposed individuals who inherit the 'at risk' genotypes of xenobiotic metabolizing enzymes⁹. Indeed, studies have associated an increased risk of lung cancer with the induction of aryl hydrocarbon hydroxylase and/or polymorphisms in CYP1A1 (ref. 10). Although β -carotene is known to increase

the levels of phase II detoxifying enzymes such as glutathione *S*-transferase Mu and glutathione peroxidase enzymes, smokers with the CYP1A1 exon-7 valine polymorphism have significantly higher levels of PAH-DNA adduct; β -carotene intake does not significantly decrease these levels¹¹.

We used electron paramagnetic resonance to evaluate the precise contribution of CYPs induced by β -carotene on superoxide production. There was a significant association between the induction of CYP content in subcellular lung preparations and the overgeneration of superoxide yield (not shown), which could act synergistically with the peroxy radicals, nitrogen dioxide and hydroquinones that are contained in cigarette smoke. The pro-oxidant activity of β -carotene has also been unambiguously demonstrated at a high partial pressure of oxygen. Because this is highest in the outermost cells of the lung, these cells might be particularly subject to the pro-oxidant effect of β -carotene¹².

We found in a medium-term bioassay with BALB/c 3T3 cells that β -carotene enhances the conversion of the prototype benzo(*a*)pyrene to the ultimate carcinogens (our unpublished data). This co-carcinogenic activity of β -carotene is in line with the boosting effect of β -carotene itself on activating enzymes during cell growth.

Although cancer chemoprevention cannot rely merely on the control of antioxidants, there have been proposals to take advantage of the radical-trapping ability of β -carotene (and probably of other carotenoids) to try to decrease the incidence of lung cancer in humans. We postulate that the paradoxical effect of increased morbidity and mortality observed in the clinical chemoprevention trials is probably due to the co-carcinogenic properties of β -carotene and its ability to generate oxidative stress¹³. We think that our findings are relevant to public health policy and that they should be considered before widespread supplementation with these micronutrients is recommended.

M. Paolini*, **G. Cantelli-Forti***, **P. Perocco†**, **G. F. Pedullif**, **S. Z. Abdel-Rahman§**, **M. S. Legator§**

*Department of Pharmacology, Biochemical Toxicology Unit, Via Irnerio 48, 40126 Bologna, Italy
e-mail: paolini@biocfarm.unibo.it

†Institute of Cancerology, Viale Filopanti 22, 40126 Bologna, Italy

‡Department of Organic Chemistry 'A. Mangini', Via S. Donato 15, 40127 Bologna, Italy

§Department of Preventive Medicine and Community Health, University of Texas Medical Branch, Galveston, Texas 77555-1110, USA

- Ziegler, R. G. *et al.* *J. Natl Cancer Inst.* **88**, 612–615 (1996).
- The α -Tocopherol, β -Carotene Cancer Prevention Study Group. *N. Engl. J. Med.* **330**, 1029–1035 (1994).

- Omenn, G. S. *et al.* *J. Natl Cancer Inst.* **88**, 1550–1558 (1996).
- Omenn, G. S. *et al.* *N. Engl. J. Med.* **334**, 1150–1155 (1996).
- Hinds, T. S., West, W. L. & Knight, E. M. *Ther. Rev.* **37**, 551–558 (1997).
- Azuine, M. A., Goswami, U. C., Kayal, J. J. & Bhide, S. V. *Nutr. Cancer* **17**, 287–295 (1992).
- Paolini, M., Biagi, G., Bauer, C. & Cantelli-Forti, G. *Trends Pharmacol. Sci.* **15**, 322–323 (1994).
- Paolini, M. *et al.* *Br. J. Pharmacol.* **122**, 344–350 (1997).
- Bartsch, H. & Hietanen, E. *Environ. Health Perspect.* **104** (suppl. 3), 569–577 (1996).
- Hayashi *et al.* *Jpn. J. Cancer Res.* **83**, 866–870 (1992).
- Mooney, L. A. *et al.* *Carcinogenesis* **18**, 503–509 (1997).
- Rice-Evans, C. A., Sampson, J., Bramley, P. M. & Holloway, D. E. *et al.* *Free Radical Res.* **26**, 381–398 (1997).
- Rowe, P. M. *Lancet* **348**, 1369 (1996).

Growth of nanotubes for probe microscopy tips

Carbon nanotubes, which have intrinsically small diameters and high aspect ratios and which buckle reversibly, make potentially ideal structures for use as tips in scanning probe microscopies, such as atomic force microscopy (AFM)^{1–4}. However, the present method of mechanically attaching nanotube bundles for tip fabrication is time consuming and selects against the smallest nanotubes, limiting the quality of tips. We have developed a technique for growing individual carbon nanotube probe tips directly, with control over the orientation, by chemical vapour deposition (CVD) from the ends of silicon tips. Tips grown in this way may become widely used in high-resolution probe microscopy imaging.

Our approach to growing individual nanotube probes involves flattening a conventional silicon (Si) tip at its apex by contact AFM imaging and anodizing it in hydrogen fluoride⁵ to create nanopores of 50–100 nm diameter along the tip axis. Iron catalyst is electrodeposited into the pores from FeSO₄ solution⁶, and nanotubes are grown by CVD with ethylene and hydrogen at 750 °C. The orientated pore structure was chosen for the catalyst support in order to control the direction of growth⁷ and enable the reproducible production of nanotube tips for imaging.

CVD nanotube tips are formed reproducibly after a reaction lasting 10 min (Fig. 1). They are usually too long to be used as tips, and are shortened by an *in situ* AFM technique^{1,2}. A typical field-emission scanning electron microscopy (FE-SEM) image of a nanotube tip after it was shortened and used for AFM imaging (Fig. 1a) shows a well-defined tube 480 nm long protruding from the Si tip apex. Nanotube tips produced under these conditions and viewed by FE-SEM have an average diameter of 10 \pm 5 nm. Further characterization of these tips by transmission electron microscopy show that they are multi-walled nanotubes (MWNs) with well-ordered graphene walls (Fig. 1b).

AFM measurements of the cantilever

oscillation amplitude versus the position above a substrate (Fig. 1c) show that these individual nanotubes buckle elastically, as observed previously for mechanically attached, arc-grown MWNTs¹. Buckling curves can be repeated many times for a given tip, demonstrating that both the nanotube and its attachment to the Si tip are robust, and can be used to verify *in situ* that the nanotube tip is used for imaging.

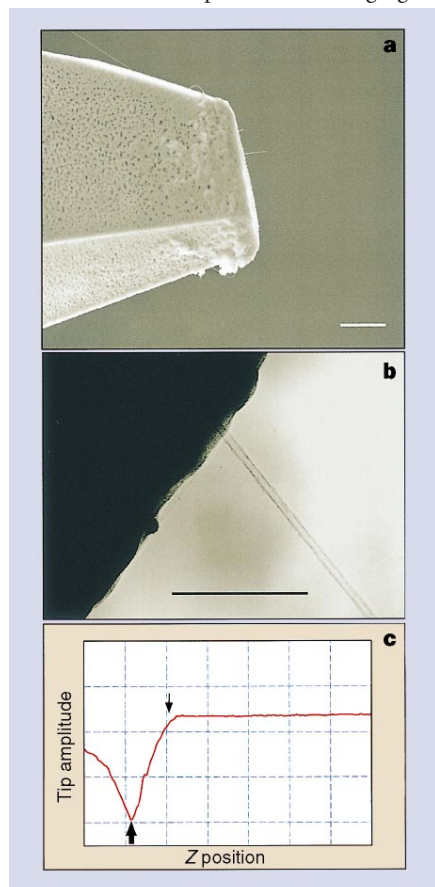


Figure 1 Characterization of CVD nanotube tips. **a**, FE-SEM image of a CVD nanotube tip that has been shortened for imaging. Nanotubes were grown from a uniform pore structure consisting of pores about 60 nm in diameter, with 150 pores per μm^2 . Scale bar, 1 μm . **b**, Transmission electron microscope (TEM) image of a CVD nanotube tip. The entire AFM cantilever/tip assembly with nanotube tip was mounted on a custom TEM holder for imaging. Scale bar, 100 nm. **c**, Tip oscillation amplitude (grid marks 5 nm apart) as a function of height above the sample (Z position; grid marks 2 nm apart) recorded in force calibration mode with a Nanoscope III (Digital Instruments). The right of the plot corresponds to free oscillation of the tip above the surface. As the tip approaches and begins to tap the surface (thin arrow), the amplitude decreases to zero. The oscillation amplitude increases again after the nanotube buckles (thick arrow). CVD nanotubes were grown in a tube furnace. Tips (with catalyst) were heated by 15 $^\circ\text{C}$ per min to 750 $^\circ\text{C}$ in a flow of 950 STP $\text{cm}^3 \text{min}^{-1}$ argon and 40 STP $\text{cm}^3 \text{min}^{-1}$ hydrogen. At 750 $^\circ\text{C}$, 10 STP $\text{cm}^3 \text{min}^{-1}$ ethylene was added for 10 min, and the furnace was cooled at 15 $^\circ\text{C}$ per min in 500 STP $\text{cm}^3 \text{min}^{-1}$ argon.

The imaging performance of CVD nanotube probes has been characterized using gold nanoparticle standards⁸ and immunoglobulin M. Gold nanoparticles with mean diameters of 2 and 5 nm were imaged on mica, and the image widths were used with a two-sphere model to estimate the tip resolution. The results show that we can routinely obtain very high-resolution tips with end radii of 3–6 nm. This is an improvement on our previous MWNT tips², our single-walled nanotube⁴ (SWNT) bundle tips, and commercial Si and Si_3N_4 tips, whose radii are generally greater than 5–10 nm. Our tips are also very robust and do not readily contaminate (in contrast to the sharpest Si and Si_3N_4 ones). They can be used several times and, when a tip ultimately fails, the carbon is removed by oxidation (at 500 $^\circ\text{C}$ for 20 min) and a new tip is grown by CVD. Tips have been through this cycle 20 times with no loss of yield or resolution.

These single nanotube tips may also be used for imaging biological macromolecules. For example, intermittent contact AFM images of IgM (Fig. 2) show excellent resolution. Routine images show the pentameric structure, including five external pairs of antigen-binding fragments and five internal crystallizable fragment domains⁹. Images occasionally exhibit a loop structure connecting two of the five domains that might correspond to the joining loop⁹. Higher-resolution AFM images have been

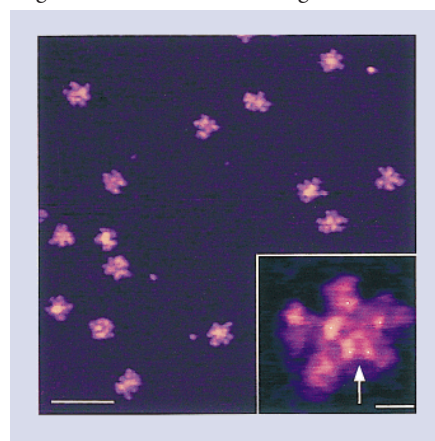


Figure 2 Imaging IgM macromolecules with a CVD nanotube tip at high resolution. Apparent structural differences in individual IgMs are due to absorption in different orientations. Molecular height ranges from 2.5 to 3.5 nm. Scale bar, 100 nm. Inset, high-resolution image of IgM. Small white dots, crystallizable Fc fragments; white arrow, possible position of the joining loop. Scale bar, 10 nm. Images were recorded in tapping mode in air with CVD nanotube tips grown on force-modulation-etched Si probes. Samples were prepared from mouse IgM (>95%, Sigma) by diluting to 2 mg ml^{-1} in 0.05 M phosphate-buffered saline solution, pH 7.0; 25 μl of the solution was dropped onto freshly cleaved mica, allowed to stand for 1 min, rinsed with water and dried with nitrogen.

reported using commercial tips^{10,11}, but only of densely packed arrays of proteins. When individual molecules have been imaged with these same tips, the resolution is lower¹¹.

Individual CVD nanotube tips routinely show higher-resolution images of isolated protein molecules than our previous results with MWNT and SWNT bundle tips (consistent with measurements on gold nanoclusters) and room-temperature AFM data with commercial tips¹², and are comparable to the high-resolution data obtained at low temperatures by cryo-AFM¹³. Our results reflect the small radii, cylindrical shape and low adhesion forces (typically less than 30 pN) of individual MWNT tips.

The high resolution of individual MWNT tips means that they could be used for imaging nanostructures and functional mapping when the ends are modified³. This CVD method also could be implemented on a large scale, making nanotube tips widely accessible. The resolution may be further improved by preparing smaller-diameter SWNT tips^{14,15}, leading to their use in many areas of biology and chemistry.

Jason H. Hafner, Chin Li Cheung, Charles M. Lieber

Department of Chemistry and Chemical Biology, Harvard University, 12 Oxford Street, Cambridge, Massachusetts 02138, USA
e-mail: cml@cmliris.harvard.edu

- Dai, H., Hafner, J. H., Rinzler, A. G., Colbert, D. T. & Smalley, R. E. *Nature* **384**, 147–150 (1996).
- Wong, S. S., Harper, J. D., Lansbury, P. T. & Lieber, C. M. *J. Am. Chem. Soc.* **120**, 603–604 (1998).
- Wong, S. S., Joselevich, E., Woolley, A. T., Cheung, C. L. & Lieber, C. M. *Nature* **394**, 52–55 (1998).
- Wong, S. S. *et al. Appl. Phys. Lett.* **73**, 3465–3467 (1998).
- Lehmann, V. *Thin Solid Films* **255**, 1–4 (1995).
- Ronkel, F., Schultze, J. W. & Arens-Fischer, R. *Thin Solid Films* **276**, 40–43 (1996).
- Li, W. Z. *et al. Science* **274**, 1701–1703 (1996).
- Vesenska, J., Manne, S., Giberson, R., Marsh, T. & Henderson, E. *Biophys. J.* **65**, 992–997 (1993).
- Perkins, S. J., Nealis, A. S., Sutton, B. J. & Feinstein, A. *J. Mol. Biol.* **221**, 1345–1366 (1991).
- Shao, Z., Mou, J., Czajkowsky, D. M., Yang, J. & Yuan, J.-Y. *Adv. Phys.* **45**, 1–86 (1996).
- Muller, D., Amrein, M. & Engel, A. *J. Struct. Biol.* **119**, 172–188 (1997).
- Fritz, J., Anselmetti, D., Jarchow, J. & Fernandez-Busquets, X. *J. Struct. Biol.* **119**, 165–171 (1997).
- Zhang, Y., Sheng, S. & Shao, Z. *Biophys. J.* **71**, 2168–2176 (1996).
- Kong, J., Soh, H. T., Cassell, A. M., Quate, C. F. & Dai, H. *Nature* **395**, 878–881 (1998).
- Hafner, J. H. *et al. Chem. Phys. Lett.* **296**, 195–202 (1998).

scientific correspondence is intended to provide a forum for both brief, topical reports of general scientific interest and technical discussion of recently published material of particular interest to non-specialist readers. Priority will be given to contributions that have fewer than 500 words, 10 references and only one figure. Detailed guidelines are available on *Nature's* website (www.nature.com) or on request from nature@nature.com